


# Screening of 1,3,4-Thiadiazole Derivatives by *in silico* Molecular Docking to Target Estrogen Receptor for Breast Cancer

Umapathy Vanitha <sup>1</sup>, Ramakrishnan Elancheran <sup>1</sup>, Senthamarai Kannan Kabilan <sup>1</sup>, Kuppusamy Krishnasamy <sup>1,\*</sup> 

<sup>1</sup> Department of Chemistry, Annamalai University, Annamalai Nagar - 608002, Tamilnadu, India

\* Correspondence: [krishnasamybala56@gmail.com](mailto:krishnasamybala56@gmail.com) (K.K.);

Scopus Author ID: 17346420400

Received: 21.01.2022; Accepted: 4.03.2022; Published: 28.03.2022

**Abstract:** Estrogen receptor plays a key role in physiological functions and is activated by estrogens. Breast cancer is the leading cancer among women all over the world. The molecular docking research began with the use of Schrödinger software to find the lead molecule from the 1,3,4-thiadiazole derivatives. Also, ADME drug-likeness properties were predicted to find a suitable lead candidate. Out of fifty 1,3,4-thiadiazole derivatives, TOH62 and TF62 showed the highest binding energies, and gscores are -9.36 and -8.85 kcal/mol, respectively. These results proved that the phenolic OH has a certain role in the binding with the targeted protein and is responsible for the activity. In the near future, we are willing to do the *in-vitro* and *in-vivo* anti-breast cancer evaluation of these compounds.

**Keywords:** ER; thiadiazole; virtual screening; molecular docking.

**List of abbreviations:** ER = Estrogen Receptor; LBD = Ligand binding Domain; DBD = DNA-binding Domain; NTD = Non-terminal Binding Domain; SP = Standard Precision; XP = Extra Precision; TC1 = (Z)-2-(((5-(4-chlorophenyl)-1,3,4-thiadiazol-2-yl)imino)methyl)phenol derivatives; TF = (Z)-2-(((5-(4-fluorophenyl)-1,3,4-thiadiazol-2-yl)imino)methyl)phenol derivatives; TC = (Z)-2-(((5-(4-fluorophenyl)-1,3,4-thiadiazol-2-yl)imino)methyl)phenol derivatives; TOC = (Z)-2-(((5-(4-methoxyphenyl)-1,3,4-thiadiazol-2-yl)imino)methyl)phenol derivatives; TV = (Z)-4-(5-((2-hydroxybenzylidene)amino)-1,3,4-thiadiazol-2-yl)-2-methoxyphenol derivatives; TPN = (Z)-2-(((5-(4-nitrophenyl)-1,3,4-thiadiazol-2-yl)imino)methyl)phenol derivatives; TMN = (Z)-2-(((5-(3-nitrophenyl)-1,3,4-thiadiazol-2-yl)imino)methyl)phenol derivatives; TOH = (Z)-2-(((5-(4-chlorophenyl)-1,3,4-thiadiazol-2-yl)imino)methyl)phenol derivatives.

© 2022 by the authors. This article is an open-access article distributed under the terms and conditions of the Creative Commons Attribution (CC BY) license (<https://creativecommons.org/licenses/by/4.0/>).

## 1. Introduction

Cancer is a deadly abnormal cell by immortal and uncontrolled cell death. Breast cancer affects the morphology of ordinary mammary epithelial cells and is incredibly diverse and one of the leading causes of the disease in women worldwide [1]. In 2021, women in the United States were predicted to be diagnosed with 281,550 new instances of invasive breast cancer and 49,290 new cases of non-invasive (in situ) breast cancer [2]. Estrogen Receptor (ER) is one of the targets to treat breast cancer. The major heterocyclic compounds containing nitrogen, oxygen and sulfur have anticancer activities such as 1,3-thiazolidine-2,4-diones [3], 5-phenyl-1,3,4-oxadiazoles [4], 2-(4-phenylthiazol-2-yl) isoindoline-1,3-diones [5], oxobenzimidazoles [6], etc. Also, 2-thioxoimidazolidinones are known as thiohydantoin derivatives, which belong to the heterocyclic family having several biological activities such as antitumor, antibacterial, antidiabetic, anti-inflammatory, etc. [7].

Elbadawi *et al.* reported that 3,5-disubstituted-2-thiohydantoin showed very good anti-breast cancer activities, especially in MCF-7 cell lines, and also have the activity against prostate cancer cell line PC-3 [8]. Even thiadiazoles have four different isomeric positions such as 1,2,3-thiadiazole, 1,2,4-thiadiazole, 1,3,4-thiadiazole and 1,2,5-thiadiazole. Out of these, 1,3,4-thiadiazole derivatives have several pharmacological activities such as anti-inflammatory [9], anticancer [10], antidiabetic [11], etc.

Altintop *et al.* reported that a series of N-(6-substituted benzothiazole-2-yl)-2-[(5-(arylamino)-1,3,4-thiadiazol-2-yl)thio]acetamide were determined as the promising anticancer activities against breast cancer cell line MCF-7, also having the activity in HepG2 cell line [12]. The above work encourages to do the screening of 1,3,4-thiadiazole derivatives for breast cancer targets. The pharmacological activity of the 1,3,4-thiadiazole derivatives at the estrogen receptor was determined using the Schrödinger (Maestro 9.5) software.

## 2. Materials and Methods

### 2.1. Docking.

The ligands, 1,3,4-thiadiazoles were designed by changing the functional group and the substitutions, then LigPrep (v3.1), Schrödinger software suite was used to prepare the high-resolution 3D structure of the respective ligands, which include the 2D to 3D conversion, optimization, minimization of energy states, some of the other corrections [13]. The protein structure (PDB: 3ERT) was downloaded from the PDB databank, which has the estrogen receptor cocrystallized with 4-hydroxytamoxifen. The protein preparation wizard was used to refine the protein structure [14] then the Receptor grid was generated using Receptor grid generation in Schrödinger software suite, LLC, NY, USA, 2015 [15,16]. The docking was carried out using the extra precision method (XP). The Glide score (Gscore) was calculated using the following formula in kcal/mol.

$$\text{G Score} = a \cdot \text{vdW} + b \cdot \text{Coul} + \text{Lipo} + \text{Hbond} + \text{Metal} + \text{BuryP} + \text{RotB} + \text{Site} \quad (1)$$

where Van der Waals energy is represented by vdW, with coefficients  $a=0.065$  and  $b=0.130$ . Coul is the symbol for Coulomb energy. Lipo is a symbol of lipophilic interaction. Metal-binding is represented by Metal, and hydrogen bonding is represented by H-bond. BuryP represents the penalty for buried polar groups, while RotB represents the penalty for freezing rotatable bonds. The site represents polar interactions at the active site. The computational experiments were run using a Linux operating system [17].

### 2.2. ADME properties.

By use of the QikProp, which provides physically significant descriptors and uses them to do ADME predictions, was used to determine a set of ADME-related parameters of the ligands. The methods were carried out using the logarithm of aqueous solubility,  $\log \text{Swat}$  (range for 95 percent of drugs: -6.0 to 0.5); the integer of assumed binding constant to human serum albumin,  $\log \text{KHSA}$  (range for 95 percent of drugs: -1.5 to 1.2); and the integer of assumed blood/brain barrier partition coefficient,  $\log \text{B/B}$  (range for 95 percent of drugs: -1.5 to 1.2). (range for 95 percent of drugs: -3.0 to 1.0) the evident Madin-Darby canine kidney (MDCK) cell permeability in  $\text{nm s}^{-1}$  ( $25 > 500$  great); the index of cohesion interplay in solids, Indcoh, determined from the predicted Polarizability, QP polrz; the IC50 value for blocking

HERG K<sup>+</sup> channels, log HERG; the apparent Caco-2 cell permeability, QPP Caco in nm/s, metabolic reactions, #metab, Polarizability, QP polrz, etc. The ADME/T features of the finest ligands molecules were predicted using the Schrödinger 2013 QikProp tool. The number of Hydrogen Bond Acceptors (HBA) and Donors (HBD), QP log Po/w, skin permeability; log Kp, the percentage of human oral absorption, and other attributes were expected [18, 19].

### 3. Results and Discussion

In this study, 1,3,4- thiadiazole derivatives were used in *in-silico* molecular docking investigations [17]. The selected ligands (50 different derivatives of 1,3,4-thiadiazole) were docked with the estrogen receptor protein (PDB: 3ERT). The thiadiazole derivatives were screened with ER to have a deeper insight into various chemical binding modes. The interaction between the best compounds of thiadiazole derivatives and ER receptor are shown in Figure 1. Molecular docking study suggests that electron-withdrawing group like CN group has strong H-bonding with the amino acid residue ARG 394; likewise, electron-donating group like OH group has strong H-bonding with ASP 351, GLU 353, GLY 521 and HID 524. Maruthanila *et al.* also reported that the amino acid residues GLU 353, and ARG 394 are the important H-bonding sides and are also responsible for the activity and binding energies. The 2D and 3D interactions of foremost thiadiazole derivatives are shown in Figure 1.

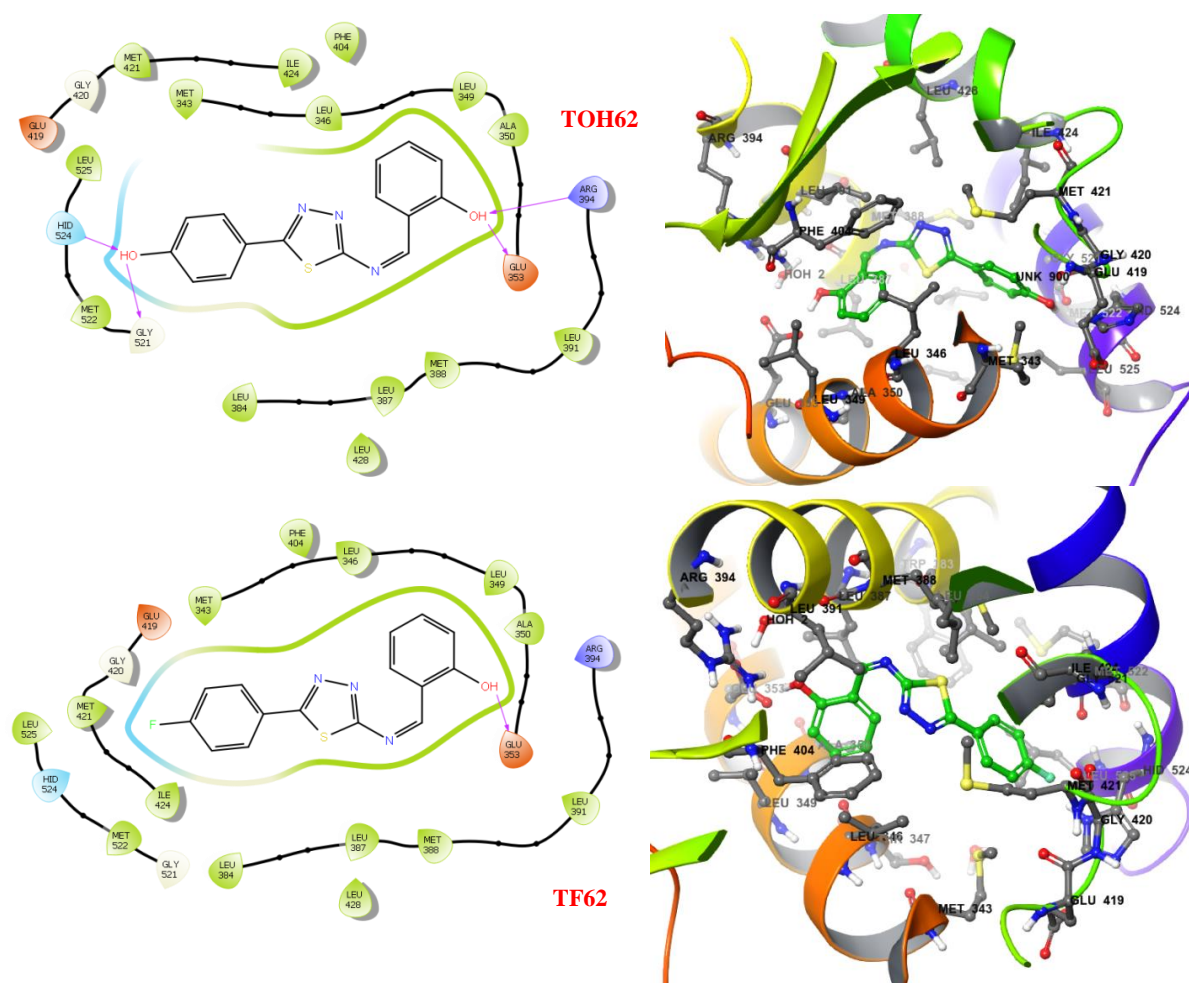


**Figure 1.** 2D and 3D interactions of foremost thiadiazole derivatives, TOH62 and TF62.

Take a look at the thiadiazole derivatives shown above, TOH62 and TF62 have shown the H-bonding between the phenolic OH and ARG 394, GLY 521, HID 524, and GLU 353

residues and also have the highest glide score (-9.36 and -8.85 kcal/mol, respectively) among the series. Also, these highlighted the hydrophobic interactions which are partially contributing to the binding affinity. Table 1 shows the lowest binding energies for the ligand-ER interaction identified. Sakkiah *et al.* reported that OHT binds ER more strongly in the antagonist conformer, whereas E2 prefers the agonist conformer, according to the binding interaction energy analysis [20]. The most stable interactions in the ERalpha OHT complex include the hydrogen bond between OHT and GLU353 and the hydrophobic interaction between OHT and ALA350 and LEU525, according to the binding interaction analysis. Because the active region of ER is mainly hydrophobic, selective binding of potential anti-breast cancer targeted therapies should rely mostly on these hydrophobic and H-bond interactions. The van der Waals interactions with the surrounding hydrophobic residues LEU 346, ILE 424, ALA 350, LEU 387, LEU 384, LEU 388, and LEU 391 were identified by docking studies. The OH and CN groups are also required for the compound's active interaction with the receptor.

**Table 1.** The lowest binding energies for the ligand-ER interaction.

Comp.	Ligand	G Score	Lipophilic Ewdw	Phoben	Hbond	Electro	Site map	Low MW	Rot Penal
1	TOH62	-9.36	-4.11	-2.48	-1.15	-1.02	-0.29	-0.5	0.19
2	TF62	-8.85	-4.7	-1.95	-0.7	-0.79	-0.4	-0.5	0.18
3	TF63	-8.85	-4.7	-1.95	-0.7	-0.79	-0.4	-0.5	0.18
4	TOH55	-8.84	-4.41	-2.44	-0.67	-0.39	-0.7	-0.48	0.25
5	TV46	-8.79	-5.52	-2.7	-0.48	-0.07	-0.31	-0.13	0.15
6	TOH52	-8.73	-3.53	-1.61	-1.65	-1.42	-0.24	-0.46	0.17
7	TOH48	-8.7	-4.84	-2.31	-0.64	-0.29	-0.4	-0.5	0.28
8	TV30	-8.66	-3.62	-2.33	-1.53	-0.18	-1.11	-0.24	0.17
9	TV33	-8.66	-3.62	-2.33	-1.53	-0.18	-1.11	-0.24	0.17
10	TV61	-8.66	-4.52	-1.45	-1.41	-0.84	-0.27	-0.31	0.13
11	TCI55	-8.53	-4.76	-2.4	-0.35	-0.1	-0.73	-0.42	0.23
12	TV45	-8.48	-4.69	-1.82	-1.31	-0.33	-0.27	-0.24	0.17
13	TOC55	-8.45	-4.73	-2.35	-0.35	-0.12	-0.73	-0.43	0.23
14	TV55	-8.44	-4.18	-2.23	-0.87	-0.41	-0.59	-0.38	0.21
15	TOH47	-8.39	-4.77	-2.07	-0.66	-0.29	-0.4	-0.5	0.31
16	TF55	-8.38	-4.6	-2.43	-0.34	-0.09	-0.71	-0.47	0.25
17	TC55	-8.34	-4.68	-2.3	-0.35	-0.07	-0.71	-0.49	0.26
18	TCI61	-8.34	-5.11	-1.55	-0.66	-0.45	-0.37	-0.35	0.14
19	TOH61	-8.32	-4.69	-1.77	-0.68	-0.64	-0.29	-0.41	0.16
20	TC61	-8.3	-5.03	-1.58	-0.62	-0.43	-0.38	-0.42	0.16
21	TV57	-8.29	-4.65	-2.15	-0.48	-0.54	-0.34	-0.33	0.2
22	TV29	-8.28	-3.91	-2.62	-0.48	-0.18	-1.03	-0.24	0.17
23	TV40	-8.22	-4.9	-1.8	-0.96	-0.3	-0.27	-0.2	0.16
24	TOC49	-8.19	-4.5	-2.7	-0.44	-0.12	-0.28	-0.35	0.2
25	TF61	-8.16	-5.01	-1.8	-0.43	-0.33	-0.34	-0.4	0.16
26	TV50	-8.15	-3.35	-1.39	-1.65	-1.26	-0.24	-0.41	0.16
27	TPN55	-8.14	-4.76	-2.09	-0.35	-0.06	-0.71	-0.38	0.22
28	TV28	-8.1	-3.56	-1.96	-0.96	-0.31	-1.24	-0.24	0.17
29	TMN55	-8.06	-4.35	-2.54	-0.35	-0.05	-0.61	-0.38	0.22
30	TV32	-8.05	-3.54	-2.22	-1.46	-0.06	-0.62	-0.38	0.21
31	TOH41	-8.03	-4.51	-2.47	-0.32	-0.23	-0.36	-0.34	0.2
32	TMN46	-8.01	-5.4	-2.7	0	-0.08	-0.31	-0.13	0.15
33	TPN46	-8	-5.44	-2.7	0	-0.14	-0.32	-0.13	0.15
34	TV52	-8	-3.49	-1.3	-1.71	-1.19	-0.22	-0.36	0.14
35	TF42	-7.96	-4.77	-2.4	0	-0.09	-0.52	-0.42	0.23
36	TOC41	-7.96	-5.12	-2.13	0	0.08	-0.69	-0.29	0.19
37	TOH50	-7.96	-3.28	-1.37	-1.31	-1.29	-0.38	-0.5	0.19
38	TOH42	-7.94	-4.31	-2.43	-0.35	-0.35	-0.31	-0.42	0.23
39	TV42	-7.94	-4.2	-2.42	-0.48	-0.41	-0.31	-0.32	0.2
40	TC42	-7.93	-4.87	-2.43	0	-0.07	-0.37	-0.43	0.23
41	TCI42	-7.9	-4.94	-2.37	0	-0.07	-0.37	-0.36	0.21
42	TF27	-7.89	-3.85	-2.33	-1.13	-0.24	-0.26	-0.26	0.18
43	TOC42	-7.85	-4.81	-2.59	0	0.01	-0.3	-0.38	0.21
44	TV41	-7.83	-4.13	-2.49	-0.48	-0.38	-0.29	-0.24	0.17

Comp.	Ligand	G Score	Lipophilic Evdw	Phoben	Hbond	Electro	Site map	Low MW	Rot Penal
45	TF56	-7.82	-5.01	-1.93	0	-0.28	-0.4	-0.5	0.29
46	TOH45	-7.81	-5.21	-2.7	0	-0.05	-0.3	-0.23	0.17
47	TOH46	-7.81	-5.21	-2.7	0	-0.05	-0.3	-0.23	0.17
48	TC41	-7.8	-5.03	-1.87	0	-0.04	-0.73	-0.34	0.2
49	TC27	-7.68	-4.22	-2.15	-1.01	-0.21	-0.01	-0.27	0.18
50	TPN50	-7.68	-4.22	-1.77	-0.89	-0.31	-0.31	-0.41	0.23

Figure 2 represents the 2D and 3D interactions of hERLBD in complex with 1,3,4-thiadiazole compounds with CN group interactions.

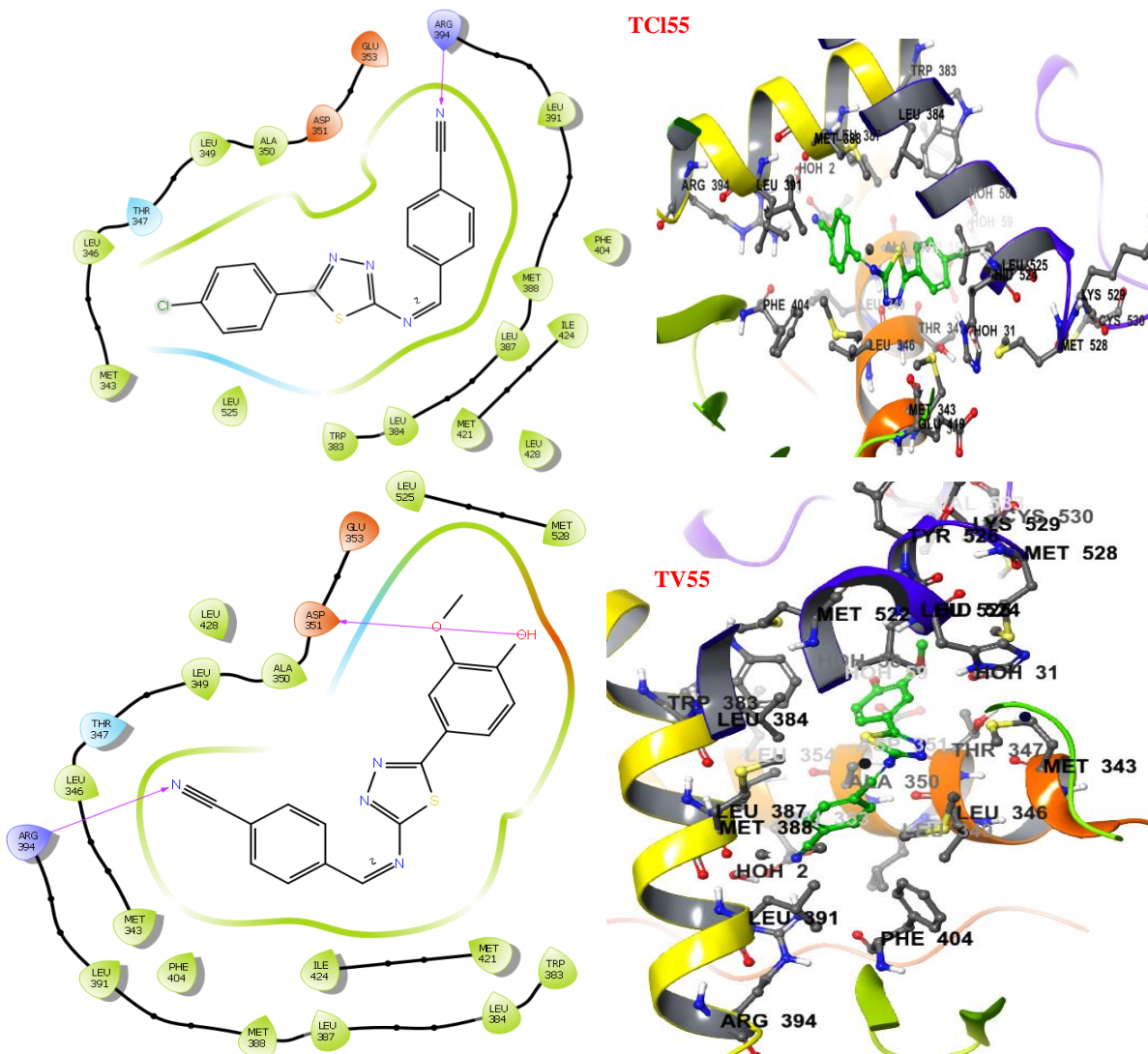


**Figure 2.** 2D and 3D interactions of foremost thiadiazole derivatives, TCI55 and TV55.

To analyze drug-likeness and pharmacokinetics parameters, we approximated the thiadiazole derivatives' absorption, distribution, metabolism, and elimination (ADME) features. ADME characteristics of the compounds are crucial descriptors for human medicinal application. For the evaluation of crucial ADME characteristics and their allowed ranges, the QikProp (Schrödinger, Inc., New York, NY, 2013) was utilized [19]. The typical range of Lipinski's rule of five for oral availability was achieved for all derivatives (Table 2). Further pharmacophore models can be utilized for comparing the screened compounds to the recorded compounds [21].

**Table 2.** Prediction of Lipinski's Rule of five for the test compounds <sup>a</sup>.

S. NO	Comp.	MW (>500)	Donor HB (<=5)	Accept HB (<=10)	QP polrz	QP logPw	QP logPo /w(<5)
1	TOH62	297.331	2	4.5	30.573	10.616	2.395
2	TF62	299.322	1	3.75	30.948	8.29	3.424
3	TF63	299.322	1	3.75	30.967	8.296	3.428
4	TOH55	306.341	1	5.25	32.364	10.133	2.24
5	TV46	411.477	1	4.5	45.394	10.16	5.249
6	TOH52	313.33	3	5.25	30.453	12.705	1.709
7	TOH48	287.354	1	3.75	28.866	8.089	3.017
8	TV30	379.356	1	4.5	36.567	8.761	4.332
9	TV33	379.356	1	4.5	36.567	8.761	4.332
10	TV61	357.383	2	6	34.542	11.086	2.704
11	TCI55	324.787	0	4.5	33.802	7.795	3.432
12	TV45	377.417	2	5.25	39.608	11.72	3.682
13	TOC55	320.368	0	5.25	34.344	8.269	2.989
14	TV55	336.367	1	6	34.263	10.362	2.51
15	TOH47	271.293	1	4.25	27.471	8.637	2.397
16	TF55	308.332	0	4.5	32.788	7.817	3.17
17	TC55	304.369	0	4.5	34.375	7.734	3.256
18	TCI61	345.803	1	4.5	34.108	8.524	3.794
19	TOH61	327.357	2	5.25	32.643	10.859	2.537
20	TC61	325.384	1	4.5	34.638	8.46	3.548
21	TV57	350.394	2	4.5	36.27	10.673	3.431
22	TV29	379.356	1	4.5	36.88	8.702	4.418
23	TV40	391.444	1	5.25	41.636	9.856	4.478
24	TOC49	345.418	0	3.75	39.607	7.528	4.953
25	TF61	329.348	1	4.5	33.088	8.546	3.538
26	TV50	327.357	2	5.25	32.508	10.853	2.537
27	TPN55	335.339	0	5.5	34.226	9.156	2.178
28	TV28	379.356	1	4.5	36.85	8.698	4.412
29	TMN55	335.339	0	5.5	34.183	9.151	2.17
30	TV32	336.367	1	6	35.249	10.594	2.682
31	TOH41	349.33	1	3.75	33.974	8.239	4.114
32	TMN46	410.449	0	4	45.28	8.943	5.063
33	TPN46	410.449	0	4	45.353	8.954	5.076
34	TV52	343.356	3	6	32.378	12.934	1.859
35	TF42	325.403	0	3	36.527	5.656	5.028
36	TOC41	363.357	0	3.75	35.976	6.376	4.841
37	TOH50	297.331	2	4.5	30.573	10.616	2.395
38	TOH42	323.412	1	3.75	36.102	7.973	4.107
39	TV42	353.438	1	4.5	38.007	8.202	4.233
40	TC42	321.439	0	3	38.016	5.553	5.093
41	TCI42	341.857	0	3	37.557	5.636	5.293
42	TF27	373.401	0	5.25	37.993	7.217	4.427
43	TOC42	337.439	0	3.75	38.123	6.123	4.832
44	TV41	379.356	1	4.5	35.911	8.472	4.248
45	TF56	284.31	0	4	30.788	7.192	3.387
46	TOH45	381.451	1	3.75	43.5	9.931	5.129
47	TOH46	381.451	1	3.75	43.5	9.931	5.129
48	TC41	347.357	0	3	35.988	5.84	5.102
49	TC27	369.437	0	5.25	39.55	7.132	4.508
50	TPN50	326.329	1	4.75	32.498	9.642	2.473

<sup>a</sup>All values are calculated by QikProp v3.5, and the explanations of the descriptors are given in the text.

The computed log p (octanol-water partition coefficient), which has been implicated in logBB (blood-brain barrier) penetration and permeability investigations, was used to screen active and ADME compliant thiadiazole derivatives. The generated descriptors were used to evaluate the distribution of each derivative in a human (Table 3). The ADME parameters are quite comparable to those of the standard, and they fall within the usual range of values for 95% of all known medicines [21, 22].

The glide score is an indirect measure of the ligand-receptor interaction's binding free energy: the stronger the interaction, the more negative the glide score [23]. The majority of

breast cancers nowadays are ER-positive. Chemotherapy is less successful in patients with ER-positive breast cancer than in those with ER-negative illness. The binding energy and explanation are important discoveries for future experimental and theoretical investigation [24].

**Table 3.** Calculated pharmacokinetics parameters for the test compounds<sup>a</sup>.

S. NO	Comp.	QP Log HERG	QPP Caco	QP logBB	QPP MDCK	QP logKp	#metab	QP Log Khsa	Percent Human Oral Absorption
1	TOH62	-5.67	328.523	-1.121	227.663	-2.745	3	0.006	86.343
2	TF62	-5.671	1091.312	-0.426	1510.249	-1.812	2	0.208	100
3	TF63	-5.671	1091.312	-0.426	1510.249	-1.812	2	0.208	100
4	TOH55	-5.925	185.596	-1.433	123.144	-3.228	2	0.013	80.662
5	TV46	-7.203	1036.255	-0.758	808.964	-1.281	3	0.936	100
6	TOH52	-5.54	96.194	-1.736	60.194	-3.844	4	-0.149	72.447
7	TOH48	-5.427	796.852	-0.547	1094.216	-2.211	3	0.093	96.541
8	TV30	-6.057	1041.57	-0.443	3187.954	-1.917	4	0.457	100
9	TV33	-6.057	1041.57	-0.443	3187.954	-1.917	4	0.457	100
10	TV61	-5.505	320.093	-1.336	222.038	-2.968	5	0.065	87.62
11	TCI55	-5.974	614.904	-0.615	1109.713	-2.331	1	0.103	96.956
12	TV45	-6.66	376.727	-1.284	277.597	-2.363	4	0.407	94.608
13	TOC55	-5.959	614.696	-0.916	450.047	-2.262	2	-0.049	94.36
14	TV55	-5.825	198.958	-1.503	131.817	-3.257	3	0.02	82.783
15	TOH47	-5.292	750.013	-0.658	557.936	-2.206	3	-0.094	92.437
16	TF55	-5.931	614.919	-0.718	814.658	-2.297	1	0.023	95.419
17	TC55	-5.981	614.683	-0.859	449.847	-2.361	2	0.15	95.92
18	TCI61	-5.654	978.915	-0.518	1844.343	-2.051	3	0.313	100
19	TOH61	-5.6	298.106	-1.27	206.717	-2.94	4	0.046	86.29
20	TC61	-5.653	971.986	-0.704	740.572	-2.88	4	0.353	100
21	TV57	-6.032	459.427	-1.052	326.841	-2.467	3	0.363	94.682
22	TV29	-60.97	1016.964	-0.444	3566.144	-1.985	4	0.485	100
23	TV40	-6.673	1017.339	-0.825	814.763	-1.607	4	0.6	100
24	TOC49	-6.863	3125.894	-0.128	2745.709	-0.512	2	0.637	100
25	TF61	-5.608	978.449	-0.564	1351.333	-2.017	3	0.241	100
26	TV50	-5.567	288.135	-1.282	196.035	-2.974	4	0.039	85.821
27	TPN55	-5.996	73.761	-1.894	45.526	-4.063	2	-0.122	73.131
28	TV28	-6.086	1016.778	-0.444	3548.102	-1.987	3	0.483	100
29	TMN55	-5.983	73.423	-1.894	45.193	-4.07	2	-0.125	73.044
30	TV32	-6.232	211.482	-1.537	149.027	-3.101	3	0.057	84.266
31	TOH41	-5.786	896.994	-0.383	2958.037	-2.108	2	0.428	100
32	TMN46	-7.36	381.756	-1.183	278	-2.098	2	0.944	89.844
33	TPN46	-7.377	381.478	-1.186	278.802	-2.095	2	0.949	89.91
34	TV52	-5.456	104.296	-1.81	65.46	-3.862	5	-0.119	73.954
35	TF42	-5.894	2979.118	-0.029	4492.535	-1.125	2	0.727	100
36	TOC41	-5.835	2966.887	0.145	10000	-1.143	2	-0.125	73.044
37	TOH50	-5.635	270.394	-1.208	183.731	-2.942	3	0.013	84.499
38	TOH42	-5.886	895.136	-0.758	675.267	-2.061	3	0.58	100
39	TV42	-5.785	959.201	-0.813	721.711	-2.09	4	0.593	100
40	TC42	-5.886	2926.535	-0.161	2426.818	-1.214	3	0.849	100
41	TCI42	-5.936	2977.243	0.024	6123.888	-1.16	2	0.808	100
42	TF27	-5.97	3106.823	-0.145	4945.329	-1.059	4	0.271	100
43	TOC42	-5.935	2776.762	-0.249	2291.896	-1.155	3	0.659	100
44	TV41	-5.702	962.847	-0.438	3192.549	-2.135	3	0.444	100
45	TF56	-5.775	2255977	-0.053	3331.607	-1.221	2	-0.008	100
46	TOH45	-7.325	966.31	-0.707	760.62	-1.253	2	0.925	100
47	TOH46	-7.325	966.31	-0.707	760.62	-1.253	2	0.925	100
48	TC41	-5.844	2961.332	0.202	10000	-1.244	2	0.687	100
49	TC27	-6.004	3104.02	-0.271	2727.788	-1.124	5	0.397	100
50	TPN50	-5.753	114.189	-1.629	73.447	-3.716	3	0.133	78.256

Molecular dynamics investigations support the docking findings, demonstrating that, in addition to hydrophobic and  $\pi$ - $\pi$  stacking interactions, H-bond contact with ARG394 drives binding within LBD [25, 26]. These docking results significantly impact the experimental

cytotoxicity of the compounds [27-30]. This study could be used as a lead molecule to further reasonably optimize the structure of anti-estrogen drugs with stronger binding and higher activity in DBD [31-33].

#### 4. Conclusions

In this study, 3ERT was targeted using a logical method based on the in-silico predictive potential to find the lead molecule for breast cancer. The study took advantage of the power of binding affinity and physiologically significant interactions. Docking analyses were carried out after the screened compounds were compared to standard compounds. The docking results revealed significant affinity with the estrogen receptor as well as identical binding interactions with native cocrystallized ligands of the specific receptor.

#### Funding

Dr. R.Elancheran thanked DST-PURSE phase II for the financial support. Prof. S. Kabilan and U. Vanitha thank University Grants Commission, New Delhi, for the UGC BSR Faculty Fellowship.

#### Acknowledgments

The authors are thankful to the Vice-Chancellor, Annamalai University, for giving us the facility to carry out this work.

#### Conflicts of Interest

The authors confirm that this article's content has no conflict of interest.

#### References

1. Sharma, R.; Jaitak, V. Asparagus racemosus (Shatavari) targeting estrogen receptor  $\alpha$ : An in-vitro and in-silico mechanistic study. *Natural Product Research* **2020**, *34*, 1571-4, <https://doi.org/10.1080/14786419.2018.1517123>.
2. Newton, R.U.; Taaffe, D.R.; Spry, N.; Gardiner, R.A.; Levin, G.; Wall, B.; Joseph, D.; Chambers, S.K.; Galvão, D.A. A phase III clinical trial of exercise modalities on treatment side-effects in men receiving therapy for prostate cancer. *BMC cancer* **2009**, *9*, 1-8, <https://doi.org/10.1186/1471-2407-9-210>.
3. Elancheran, R.; Saravanan, K.; Divakar, S.; Kumari, S.; Maruthanila, V.L.; Kabilan, S.; Ramanathan, M.; Devi, R.; Kotoky, J. Design, synthesis and biological evaluation of novel 1, 3-thiazolidine-2, 4-diones as anti-prostate cancer agents. *Anti-Cancer Agents Med. Chem.* **2017**, *17*, 1756-68, <https://doi.org/10.2174/1871521409666170412121820>.
4. Ananth, A.H.; Manikandan, N.; Rajan, R.K.; Elancheran, R.; Lakshmithendral, K.; Ramanathan, M.; Bhattacharjee, A.; Kabilan, S. Design, Synthesis, and Biological Evaluation of 2-(2-Bromo-3-nitrophenyl)-5-phenyl-1, 3, 4-oxadiazole Derivatives as Possible Anti-Breast Cancer Agents. *Chem Biodivers.* **2020**, *17*, e1900659, <https://doi.org/10.1002/cbdv.201900659>.
5. Saravanan, K.; Elancheran, R.; Divakar, S.; Anand, S.A.A.; Ramanathan, M.; Kotoky, J.; Lokanath, N.K.; Kabilan, S. Design, synthesis and biological evaluation of 2-(4-phenylthiazol-2-yl) isoindoline-1, 3-dione derivatives as anti-prostate cancer agents. *Bioorg. Med. Chem. Lett.* **2017**, *27*, 1199-204, <https://doi.org/10.1016/j.bmcl.2017.01.065>.
6. Elancheran, R.; Saravanan, K.; Choudhury, B.; Divakar, S.; Kabilan, S.; Ramanathan, M.; Das, B.; Devi, R.; Kotoky, J. Design and development of oxobenzimidazoles as novel androgen receptor antagonists. *Med. Chem. Res.* **2016**, *25*, 539-52, <https://doi.org/10.1007/s00044-016-1504-3>.



7. Vanitha, U.; Elancheran, R.; Manikandan, V.; Kabilan, S.; Krishnasamy, K. Design, synthesis, characterization, molecular docking and computational studies of 3-phenyl-2-thioxoimidazolidin-4-one derivatives. *J. Mol. Struc.* **2021**, *1246*, 131212, <https://doi.org/10.1016/j.molstruc.2021.131212>.
8. Elbadawi, M.M.; Khodair, A.I.; Awad, M.K.; Kassab, S.E.; Elsaady, M.T.; Abdellatif, K.R. Design, synthesis and biological evaluation of novel thiohydantoin derivatives as antiproliferative agents: A combined experimental and theoretical assessments. *J. Mol. Struc.* **2022**, *1249*, 131574, <https://doi.org/10.1016/j.molstruc.2021.131574>.
9. Hafez, H.N.; Hegab, M.I.; Ahmed-Farag, I.S.; El-Gazzar, A.B.A. A facile regioselective synthesis of novel spiro-thioxanthene and spiro-xanthene-9', 2-[1, 3, 4] thiadiazole derivatives as potential analgesic and anti-inflammatory agents. *Bioorg. Med. Chem. Lett.* **2008**, *18*, 4538-43, <https://doi.org/10.1016/j.bmcl.2008.07.042>.
10. Janowska, S.; Paneth, A.; Wujec, M. Cytotoxic Properties of 1, 3, 4-Thiadiazole Derivatives—A Review. *Molecules* **2020**, *25*, 4309, <https://doi.org/10.3390/molecules25184309>.
11. Datar, P.A.; Deokule, T.A. Design and synthesis of thiadiazole derivatives as antidiabetic agents. *Med. Chem.* **2014**, *4*, 390-9, <https://doi.org/10.4172/2161-0444.1000170>.
12. Altıntop, M.D.; Sever, B.; Özdemir, A.; Ilgin, S.; Atlı, Ö.; Turan-Zitouni, G.; Kaplancıklı, Z.A. Synthesis and evaluation of a series of 1, 3, 4-thiadiazole derivatives as potential anticancer agents. *Anti-Cancer Agents Med. Chem.* **2018**, *18*, 1606-16, <https://doi.org/10.2174/1871520618666180509111351>.
13. LigPrep, Schrödinger, LLC, New York, NY, **2021**.
14. Protein Preparation Wizard; Epik, Schrödinger, LLC, New York, NY, **2021**; Impact, Schrödinger, LLC, New York, NY; Prime, Schrödinger, LLC, New York, NY, **2021**.
15. Glide, Schrödinger, LLC, New York, NY, **2021**.
16. Maestro, Schrödinger, LLC, New York, NY, **2021**.
17. Maruthanila, V.L.; Elancheran, R.; Roy, N.K.; Bhattacharya, A.; Kunnumakkara, A.B.; Kabilan, S.; Kotoky, J. In silico molecular modelling of selected natural ligands and their binding features with estrogen receptor alpha. *Curr. Comput. Aided Drug Des.* **2019**, *15(1)*, 89-96, <https://doi.org/10.2174/1573409914666181008165356>.
18. Elancheran, R.; Kabilan, S.; Kotoky, J.; Ramanathan, M.; Bhattacharjee, A. In Silico Molecular Docking, Synthesis of 4-(4-benzoylamino-phenoxy) Phenol Derivatives as Androgen Receptor Antagonists. *Comb. Chem. High. Throughput Screen.* **2019**, *22(5)*, 307-16, <http://doi.org/10.2174/1386207322666190701124752>.
19. QikProp, Schrödinger, LLC, New York, NY, **2021**.
20. Sakkiah, S.; Selvaraj, C.; Guo, W.; Liu, J.; Ge, W.; Patterson, T.A.; Hong, H. Elucidation of Agonist and Antagonist Dynamic Binding Patterns in ER- $\alpha$  by Integration of Molecular Docking, Molecular Dynamics Simulations and Quantum Mechanical Calculations. *Int. J. Mol. Sci.* **2021**, *22*, 9371, <https://doi.org/10.3390/ijms22179371>.
21. Sahayarayan, J.J.; Rajan, K.S.; Vidhyavathi, R.; Nachiappan, M.; Prabhu, D.; Alfarraj, S.; Arokiyaraj, S.; Daniel, A.N. In-silico protein-ligand docking studies against the estrogen protein of breast cancer using pharmacophore based virtual screening approaches. *Saudi J. Biol. Sci.* **2021**, *28*, 400-7, <https://doi.org/10.1016/j.sjbs.2020.10.023>.
22. Rajitha, G.; Rani, M.V.; Vankadoth, U.N.; Umamaheswari, A. Design of Novel Selective Estrogen Receptor Inhibitors using Molecular Docking and Protein-Ligand Interaction Fingerprint Studies. *Int. J. Pharm. Res.* **2021**, *33*, 470-483, <https://doi.org/10.9734/JPRI/2021/v33i46A32890>.
23. Mangalath, D.L.; Mohammed, S.A.H. Ligand Binding Domain of Estrogen Receptor Alpha Preserve a Conserved Structural Architecture Similar to Bacterial Taxis Receptors. *Front. Ecol. Evol.* **2021**, *9*, 447, <https://doi.org/10.3389/fevo.2021.681913>.
24. Alamri, A.; Rauf, A.; Khalil, A.A.; Alghamdi, A.; Alafnan, A.; Alshammari, A.; Alshammari, F.; Malik, J.A.; Anwar, S. In Silico Screening of Marine Compounds as an Emerging and Promising Approach against Estrogen Receptor Alpha-Positive Breast Cancer. *Biomed Res. Int.* **2021**, <https://doi.org/10.1155/2021/9734279>.
25. Shylaja, R.; Loganathan, C.; Kabilan, S.; Vijayakumar, T.; Meganathan, C. Synthesis and evaluation of the antagonistic activity of 3-acetyl-2H-benzo [g] chromen-2-one against mutant Y537S estrogen receptor alpha via E-Pharmacophore modeling, molecular docking, molecular dynamics, and in-vitro cytotoxicity studies. *J. Mol. Struc.* **2021**, *1224*, 129289, <https://doi.org/10.1016/j.molstruc.2020.129289>.

26. Purawarga Matada, G.S.; Dhiwar, P.S.; Abbas, N.; Singh, E.; Ghara, A.; Das, A.; Bhargava, S.V. Molecular docking and molecular dynamic studies: screening of phytochemicals against EGFR, HER2, estrogen and NF-KB receptors for their potential use in breast cancer. *J. Biomol. Struct. Dyn.* **2021**, <https://doi.org/10.1080/07391102.2021.1877823>.
27. Alidmat, M.M.; Khairuddean, M.; Salhimi, S.M.; Al-Amin, M. Docking studies, synthesis, characterization, and cytotoxicity activity of new bis-chalcones derivatives. *Biomed. Res. Ther.* **2021**, *8*, 4294-306, <https://doi.org/10.15419/bmrat.v8i4.668>.
28. Dai, Y.H.; Chen, G.Y.; Tang, C.H.; Huang, W.C.; Yang, J.C.; Wu, Y.C. Drug Screening of Potential Multiple Target Inhibitors for Estrogen Receptor- $\alpha$ -positive Breast Cancer. *In vivo* **2021**, *35*(2), 761-77, <https://doi.org/10.21873/invivo.12317>.
29. Böckers, M.; Paul, N.W.; Efferth, T. Butyl octyl phthalate interacts with estrogen receptor  $\alpha$  in MCF-7 breast cancer cells to promote cancer development. *World Academy of Sciences Journal* **2021**, *3*(2), 1-1, <https://doi.org/10.3892/wasj.2021.92>.
30. Thakur, A.; Kaur, K.; Sharma, P.; Singla, R.; Singh, S.; Jaitak, V. Synthesis, In vitro, and Docking Analysis of C-3 Substituted Coumarin Analogues as Anticancer Agents. *Curr. Comput. Aided Drug Des.* **2021**, *17*(2), 161-72, <https://doi.org/10.2174/1573409916666200120114641>.
31. Cao, H.; Sun, Y.; Wang, L.; Pan, Y.; Li, Z.; Liang, Y. In silico identification of novel inhibitors targeting the DNA-binding domain of the human estrogen receptor alpha. *J. Steroid Biochem. Mol. Biol.* **2021**, *213*, 105966, <https://doi.org/10.1016/j.jsbmb.2021.105966>.
32. Cai, X.Y.; Zhang, Z.J.; Xiong, J.L.; Yang, M.; Wang, Z.T. Experimental and molecular docking studies of estrogen-like and anti-osteoporosis activity of compounds in Fructus Psoraleae. *J. Ethnopharmacol.* **2021**, *276*, 114044, <https://doi.org/10.1016/j.jep.2021.114044>.
33. Alisha, K.; Tripti, S., Repurposing statins as a potential ligand for estrogen receptor alpha via molecular docking. *Res. J. Pharm. Technol.* **2021**, *5*, 7-89, <https://doi.org/10.52711/0974-360X.2021.00650>.